A Mathematical Model of the Electrophysiological Alterations in Rat Ventricular Myocytes in Type-I Diabetes

Sandeep V. Pandit,* Wayne R. Giles,[†] and Semahat S. Demir*

*Joint Graduate Program in Biomedical Engineering, The University of Memphis, and The University of Tennessee Health Science Center, Memphis, Tennessee USA and [†]Department of Physiology and Biophysics, The University of Calgary, Calgary, Canada

ABSTRACT   Our mathematical model of the rat ventricular myocyte (Pandit et al., 2001) was utilized to explore the ionic mechanism(s) that underlie the altered electrophysiological characteristics associated with the short-term model of streptozotocin-induced, type-I diabetes. The simulations show that the observed reductions in the Ca^{2+}-independent transient outward K^+ current (I_t) and the steady-state outward K^+ current (I_{ss}), along with slowed inactivation of the L-type Ca^{2+} current (I_{CaL}), can result in the prolongation of the action potential duration, a well-known experimental finding. In addition, the model demonstrates that the slowed reactivation kinetics of I_t in diabetic myocytes can account for the more pronounced rate-dependent action potential duration prolongation in diabetes, and that a decrease in the electrogenic Na^+-K^+ pump current (I_{NaK}) results in a small depolarization in the resting membrane potential (V_{rest}). This depolarization reduces the availability of the Na^+ channels (I_{Na}), thereby resulting in a slower upstroke (dV/dt_{max}) of the diabetic action potential. Additional simulations suggest that a reduction in the magnitude of I_{CaL}, in combination with impaired sarcoplasmic reticulum uptake can lead to a decreased sarcoplasmic reticulum Ca^{2+} load. These factors contribute to characteristic abnormal $[Ca^{2+}]_i$ homeostasis (reduced peak systolic value and rate of decay) in myocytes from diabetic animals. In combination, these simulation results provide novel information and integrative insights concerning plausible ionic mechanisms for the observed changes in cardiac repolarization and excitation-contraction coupling in rat ventricular myocytes in the setting of streptozotocin-induced, type-I diabetes.

INTRODUCTION

Cardiovascular complications arising from diabetes mellitus are a leading cause of morbidity and mortality (Dillmann, 1989; Standl and Schnell, 2000). In addition to an increased incidence of coronary artery disease, the electrophysiological and the mechanical properties of the myocardium are significantly impaired (Dillmann, 1989; Mahgoub and Abdelfattah, 1998). The rat constitutes a widely utilized experimental model used to study the effects of diabetes on the heart. In an acute model of type-I (insulin deficient) diabetes, rats are injected with streptozotocin (STZ) (100 mg/kg of body wt.), and then sacrificed 4–6 days after treatment (Shimoni et al., 1994; 1995). Rat ventricular myocytes from this short-term diabetic model exhibit a prolongation of the action potential duration (APD) (Shimoni et al., 1994; 1995), along with altered intracellular Ca^{2+} homeostasis, depicted by a small reduction in the peak systolic value, and a slower decay of the intracellular Ca^{2+} transient ($[Ca^{2+}]_i$) (Ren and Davidoff, 1997). The marked delay in the final repolarization of the action potential may be responsible for the observed lengthening of the QT interval in diabetic patients (Robillon et al., 1999), and this can contribute to the enhanced incidence of cardiac arrhythmias (Ewing et al., 1991). It is therefore important to understand the ionic mechanism(s) that underlie the altered repolarization and the excitation-contraction

(E-C) coupling associated with the short-term, type-I, model of diabetes, and to gain quantitative insights into the relationship between these variables.

Experimental studies have shown that injecting STZ results in a reduction in the densities of both the Ca^{2+}-independent transient outward K^+ current (I_t), and the steady-state outward K^+ current (I_{ss}) (Shimoni et al., 1994; 1995). The subsequent decrease in the net repolarizing current is responsible for the prolongation of the APD (Shimoni et al., 1994; 1995). In contrast, the subcellular mechanisms responsible for the abnormal $[Ca^{2+}]_i$ behavior in the short-term diabetic model are not understood, although it is believed that dysfunction associated with the uptake of Ca^{2+} into the sarcoplasmic reticulum (SR) is responsible (Ren and Davidoff, 1997). Recently it was reported that freshly isolated normal adult rat ventricular myocytes maintained under cell culture conditions with hypoinsulinemia and hyperglycemia developed a phenotype (prolonged APD, slower $[Ca^{2+}]_i$ decay), somewhat similar to the one that has been described for myocytes isolated from the in vivo, short-term diabetic model (Davidoff and Ren, 1997; Ren et al., 1997). Hyperglycemic culture conditions are known to activate protein kinase C (PKC). More specifically, the ε isoform of PKC (εPKC) is activated and translocated to the sarcolemma (Malhotra et al., 2001). εPKC is the major PKC isoform in the adult rat ventricle (Bogoyevitch et al., 1993; Rybin and Steinberg, 1994). Activation of εPKC not only modulates I_t and I_{ss} (Shimoni, 1999), as is observed in the in vivo diabetic model (Shimoni et al., 1994; 1995), but has also been shown to downregulate the densities of the L-type Ca^{2+} current (I_{CaL}) (Hu et al., 2000), and the Na^+-K^+

pump current (I_{NaK}) (Buhagiar et al., 2001). Results from the available experimental studies therefore suggest that multiple interdependent ionic mechanisms (I_t, I_{ss}, I_{CaL}, I_{NaK}, and SR uptake) can mediate the electrophysiological alterations associated with this acute, type-I model of diabetes.

One approach for obtaining novel, semiquantitative insights into the complex, nonlinear interactions between different ionic mechanisms in cardiac electrophysiology is to utilize mathematical models that are based closely on experimental findings. In this way the cardiac action potential can be reconstructed, based on detailed biophysical formulations of the underlying ionic currents, pumps, and exchangers (Rudy, 2000; Winslow et al., 2000; Noble, 2002). Recently, we have developed a comprehensive mathematical model for the cardiac action potential of adult rat ventricular myocytes (Pandit et al., 2001). The equations in this model were based on biophysically derived descriptors of experimentally recorded ionic currents, pumps, and the Na^+-Ca^{2+} exchanger (I_{NaCa}) in myocytes isolated from the adult rat ventricle. The descriptions for the Ca^{2+} homeostasis mechanisms (dynamics and buffering) in the rat model were adapted (with minimal modifications) from a recent publication of Ca^{2+} handling in the canine mid-myocardial cell (Winslow et al., 1999).

The main goal of the present study was to develop a mathematical representation of the diabetic phenotype by incorporating changes in the ionic mechanisms that are suggested by experimental data to underlie the altered electrophysiological characteristics in the short-term, type-I model of STZ-induced diabetes. The model is able to qualitatively simulate the prolongation of the APD in accordance with experimental results (Fig. 1). Moreover, it provides novel insights into the ionic basis for this change in the action potential profile during diabetic conditions, and illustrates the complex, nonlinear relationship between the APD and both intracellular Ca^{2+} homeostasis, and E-C coupling.

METHODS

Mathematical model of the rat right ventricular myocyte

A mathematical model of the adult rat right ventricular (RV) cell was employed in all simulations because myocytes isolated from the RV have been utilized in most available experimental studies (Shimoni et al., 1994). This model was derived from a recently published left ventricular (LV) epicardial cell model (Pandit et al., 2001) by making modifications to the following ionic currents:

I_{Na}

The density of I_{Na} was increased by 33%. This was based on recent experimental findings, which reported a variation in the density of I_{Na} in the rat ventricle, with higher expression in RV myocytes, compared with those from the LV epicardial ones (Ashamalla et al., 2001).

I_t

The density of I_t was increased by 25%, based on reported larger values of I_t in rat RV myocytes than LV epicardium (Casis et al., 1998).
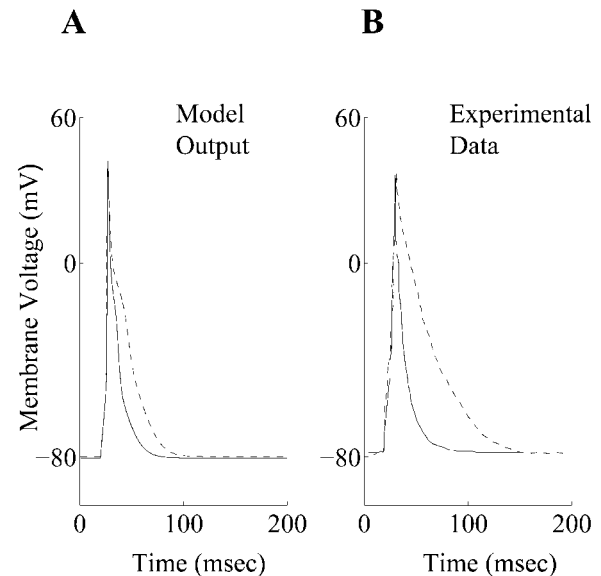

FIGURE 1 (*A*) Action potential waveforms for model generated control (*solid line*) and diabetic (*dashed line*) action potentials. (*B*) Experimentally recorded control (*solid line*) and diabetic (*dashed line*) action potentials at 1 Hz and 22°C (Shimoni et al., 1994).

I_{CaL}, I_{ss}

The densities of both I_{CaL} and I_{ss} were increased by 10%, so that the influx of Ca^{2+} ions via I_{CaL} (Q_{CaL}), and the APD_{90} value during a simulated RV action potential were comparable to corresponding experimental measurements in rat RV myocytes (Kaprielian et al., 1999; MacDonell et al., 1998) (See the Results section for a comparison of simulated and experimental values in normal RV myocytes).

A model of the rat right ventricular cell in the setting of type-I diabetes

The following modifications were made in the computational model of the normal rat RV myocyte to represent the short-term, type-I diabetic myocyte.

I_t

The density of I_t was decreased by 32%. The formulation of I_t also consists of fast and slow inactivation variables, with the relative contribution of the slow variable to overall inactivation being $\approx$11% in the normal myocyte. This was increased to $\approx$31% in the diabetic myocyte. Both of these changes are based on experimental observations that the density of I_t is reduced, and its reactivation kinetics is slower in diabetic ventricular myocytes (Shimoni et al., 1994; 1995). The simulated current-voltage (*I-V*) relationship of I_t is shown in Fig. 2 *A*, along with corresponding experimental data, which was recorded in control and diabetic RV myocytes respectively (Shimoni et al., 1994).

I_{ss}

The density of I_{ss} was decreased by 23%. Fig. 2 *B* illustrates the simulated *I-V* characteristics for I_{ss} in normal and diabetic rat RV myocytes, along with experimental data (Shimoni et al., 1994).

I_{CaL}

The density of I_{CaL} was reduced by 24%. This was based on recent experimental findings that the activation of εPKC in adult rat ventricular
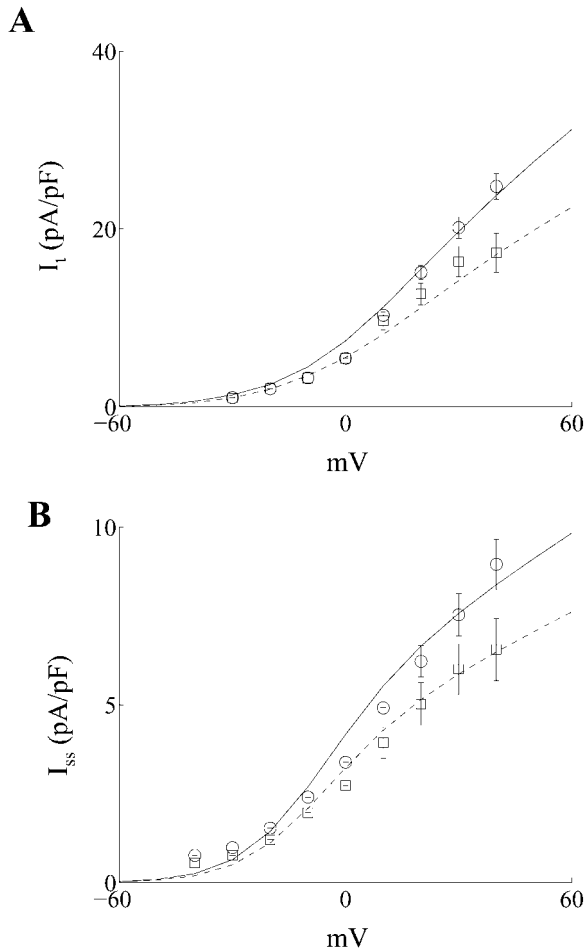
A

B

FIGURE 2 (*A*) Simulated current-voltage (*I-V*) relationship for the Ca^{2+}-independent transient outward K^+ current I_t in control ($\bigcirc$, *solid line*) and diabetic ($\square$, *dashed line*) myocytes, which were isolated from the adult rat right ventricle ($\bigcirc$, $\square$ represent experimental data from Shimoni et al., 1994). (*B*) Simulated current-voltage (*I-V*) relationship for the steady-state outward K^+ current I_{ss} in control ($\bigcirc$, *solid line*) and diabetic ($\square$, *dashed line*) myocytes, which were isolated from the adult rat right ventricle ($\bigcirc$, $\square$ represent experimental data from Shimoni et al., 1994).

myocytes reduces I_{CaL} density by $27.9 \pm 2.2\%$ (Hu et al., 2000). It has also been shown recently that the fast inactivation time constant of I_{CaL} is slowed (by $\approx 40\%$) in the chronic model of diabetes (Chattou et al., 1999). The fast inactivation time constant of I_{Cal} in our model was therefore reduced by 10%, to represent the acute diabetic conditions.

I_{NaK}

It is well-known that the Na^+-K^+-ATPase activity is decreased in STZ-induced diabetic rats (Kato et al., 1999). This was incorporated in the diabetic model by reducing the maximum density of I_{NaK} by 37%. This was based on the reported effects of εPKC on I_{NaK} density measured in rabbit ventricular myocytes (Buhagiar et al., 2001).

The changes in I_{CaL} and I_{NaK} were incorporated based on the observation that εPKC is activated and then translocated to the sarcolemmal membrane in cultured rat ventricular myocytes maintained under high extracellular glucose concentrations of 25.0 mM (Malhotra et al., 2001). This glucose level is similar to the plasma glucose concentrations recorded in the short-term, type-I, in vivo model of diabetes in rat, viz. 26.3 ± 2.15 mM (Shimoni et al., 1994).

I_{BCa}, I_{BNa}

The steady or background Ca^{2+} current (I_{BCa}) was reduced by 50% in the diabetic myocyte. This was done to maintain almost identical values of diastolic $[Ca^{2+}]_i$ during both control and diabetic simulations, in accordance with experimental findings (Ren and Davidoff, 1997). The peak magnitude of I_{BCa} during resting conditions in the control myocyte is very small (≈ 5 pA). Therefore the 50% reduction in I_{BCa} will not affect the action potential duration significantly in diabetes. Nevertheless, to compensate for a reduction of I_{BCa}, the Na^+ background current (I_{BNa}) conductance was increased by 25% in the diabetic myocyte, so that the total background current (I_B) in the range of membrane potentials near rest in both control and diabetic simulations was almost identical.

SR Ca^{2+}-ATPase

Although defects in the SR mechanisms have been well-studied in the chronic model of diabetes (Netticadan et al., 2001), very little quantitative information is available regarding these alterations in the acute model of diabetes (Ren and Davidoff, 1997). A recent study has shown that the SERCA2a protein density is decreased by $\approx 60\%$ in a chronic model of diabetes (Netticadan et al., 2001). Similarly, it is known that the affinity of Ca^{2+} ions to the SR pump is also reduced in chronic diabetes (Zhong et al., 2001). Based on these observations in the chronic model of diabetes, it has been postulated that defects in the uptake of Ca^{2+} ions into the SR also underlie the abnormal $[Ca^{2+}]_i$ behavior in short-term diabetes (Ren and Davidoff, 1997). The SR Ca^{2+}-ATPase scaling factor (K_{SR}) in the RV computational model was reduced by 45%, and the Ca^{2+}-ATPase forward rate parameter (v_{maxf}) was reduced by 20%, to represent the overall impairment in the refilling of the SR, and simulate an altered $[Ca^{2+}]_i$ similar to the one observed experimentally in short-term diabetes.

Other assumptions

The membrane capacitance (C_m) was assigned the same value (100 pF) in the control and the diabetic cell models, consistent with experimental findings (Shimoni et al., 1994). It has been recently reported that the function of the Na^+-Ca^{2+} exchanger (I_{NaCa}) is not altered in rat ventricular myocytes cultured under high glucose conditions (Dutta and Davidoff, 2000). Therefore the parameters for I_{NaCa} were similar in the control and diabetic model formulations. All other ionic mechanisms, as well as the parameters describing the SR Ca^{2+} handling were assumed to be identical in the control and the diabetic models. The extracellular ionic concentrations in both the models were assumed to be constant, and all simulations were carried out at an assumed temperature of 22°C, conditions under which most of the experimental data were recorded.

Computational aspects

The mathematical model was implemented in C, on a SUN Microsystem Sparc Ultra 60 workstation. A Runge-Kutta-Merson numerical integration algorithm, which includes an automatic step-size adjustment that is based on an error estimate, was used for the whole-cell simulations, as in our previous model studies (Demir et al., 1994, 1997, 1999; Pandit et al., 2001). The software package Matlab was also utilized in formulating model equations for the ionic channels. All the results are presented in their steady state, which was defined as the action potential obtained after allowing the model to run for 20 s after a change in the initial conditions. This approach is in accordance with earlier modeling studies examining changes in action potential and $[Ca^{2+}]_i$ profiles in pathophysiological conditions such as heart failure (Winslow et al., 1999) and atrial fibrillation (Courtemanche et al., 1999). This ensures rapid rate adaptation of the action potential, but does not take into account the long-term effects in the changes in the intracellular ionic concentrations (Courtemanche et al., 1999). The rat model requires

a run time of ~10 min on the present computing platform to simulate a steady-state action potential.

RESULTS

Action potential waveforms and underlying ionic currents in control and diabetic ventricular myocytes

A stimulus of 0.6 nA was applied for 5 ms, in accordance with experimental protocols (Ward et al., 1997), to generate the simulated control and diabetic action potentials at a frequency of 1.0 Hz and an assumed temperature of 22°C. (Fig. 1 A). The effects of the intracellular Ca^{2+} buffer EGTA in the recording pipette were included in the model in accordance with an earlier formulation (Winslow et al., 1999), because EGTA is used in majority of the electrophysiological experiments of this kind (Shimoni et al., 1994). A set of experimentally recorded action potentials under control and diabetic conditions (Shimoni et al., 1994) are shown in Fig. 1 B. The simulated control RV action potential closely resembles its experimental counterpart (Fig. 1). The simulated diabetic APD is larger than the corresponding control counterpart (Fig. 1 A) in accordance with experimental results (Fig. 1 B). However, the experimentally recorded diabetic action potential exhibits a larger prolongation (Fig. 1 B) than seen in simulations (Fig. 1 A). A quantitative comparison between the simulated and experimental diabetic action potentials was not attempted mainly because of the reportedly large variations in the duration and the shape of experimentally recorded diabetic action potentials, despite similar isolation procedures and recording conditions (e.g., see Fig. 1, B and C, in Shimoni et al., 1994). In particular, the APD_{90} value varies considerably in individual diabetic cells over time, and from cell to cell (Shimoni et al., 1998). This could be the result of variations in the magnitudes of the K^+ or background currents in diabetes (Shimoni et al., 1998), or due to the enhancement of the intrinsic action potential heterogeneity, in the rat ventricular myocardium (Watanabe et al., 1983; Ward and Giles, 1997). For these reasons, the emphasis in this modeling study was on determining whether the simulated diabetic action potential could qualitatively reproduce the experimentally observed action potential changes resulting from STZ-induced diabetes. A similar approach was successfully employed in our previous simulations, which compared and contrasted epicardial and endocardial action potentials in adult rat left ventricular myocytes (Pandit et al., 2001).

The simulated control and diabetic action potential characteristics are compared in detail in Table 1. Parameters for the simulated control RV action potential (Table 1) are very close to the corresponding experimental measurements from control myocytes, which were -80.15 ± 0.79 mV (V_{rest}), 205.6 ± 11.8 V/s (dV/dt_{max}), 40.94 ± 1.26 mV (peak overshoot), 33.27 ± 5.31 ms (APD_{90}) (All measurements

TABLE 1 Simulated action potential characteristics in control and diabetic myocytes from the rat right ventricle

	V_{rest} (mV)	R_{in} (MΩ)	dV/dt_{max} (V/s)	PO (mV)	APD_{50} (ms)	APD_{90} (ms)
Control	-80.48	71.25	182.97	41.63	14.29	31.11
Diabetic	-79.93	71.56	173.73	42.10	22.50	48.86

V_{rest}: resting membrane potential; R_{in}: input resistance; dV/dt_{max}: maximum upstroke velocity; PO: peak overshoot; APD_{50}: action potential duration (50% repolarization); APD_{90}: action potential duration (90% repolarization).

from MacDonell et al., 1998); and 62.8 ± 28.3 MΩ (R_{in}) (Shimoni et al., 1994). V_{rest}, R_{in}, and peak overshoot have similar values in the simulated control and diabetic action potentials, whereas the APD_{50} and APD_{90} are larger in the diabetic action potential; this is in qualitative agreement with experimental observations (Shimoni et al., 1994). In fact, even the small depolarization in V_{rest} (by 0.55 mV), and a small increase in R_{in} (by 0.31 MΩ) in the simulated diabetic action potential agree with the experimental observation that ''the passive properties of diabetic cells were not significantly different from those of the normal cells, although there was a tendency toward a slight depolarization of the resting potential and an increase in input resistance'' (Shimoni et al., 1994). Our model also exhibits a small reduction in dV/dt_{max} during the diabetic action potential (decreased by 5.05%), with respect to the control value.

Rate-dependent changes of the simulated cardiac action potentials at frequencies of 0.5 Hz and 2.0 Hz, in both control and diabetic cases, are shown in Fig. 3 A and B, respectively. When the stimulation rate was increased from 0.5 Hz to 2.0 Hz, the APD prolongation was more pronounced in the diabetic conditions. This agrees with experimental observations (Shimoni et al., 1994). The time- and voltage-dependent currents that primarily determine the plateau phase of the cardiac action potential in rat ventricular myocytes (I_t, I_{CaL}, I_{ss}) are shown in Fig. 4. Both I_t and I_{CaL} have smaller peak amplitudes in the diabetic case, whereas the peak magnitude of I_{ss} is almost unchanged. Overall, there is a net reduction in the outward repolarizing current, leading to a prolongation of the APD. The alteration in the I_{CaL} waveform in diabetes (smaller magnitude, slower deactivation) has important implications for dynamic changes in $[Ca^{2+}]_i$, and is discussed in the next subsection. The Na^+-K^+ pump and the Na^+-Ca^{2+} exchanger currents (I_{NaK} and I_{NaCa}, respectively), the inward rectifier K^+ current (I_{K1}), and the background current (I_B) underlying the simulated control and diabetic action potentials are shown in Fig. 5. I_{NaK} is reduced in the diabetic case. Note that I_B and I_{K1} have an altered profile; this difference between the control and diabetic conditions is primarily due to the changed contour of the action potential waveforms (the density of I_{K1} was identical in the control and the diabetic models, I_B is almost similar in control and diabetic cases).
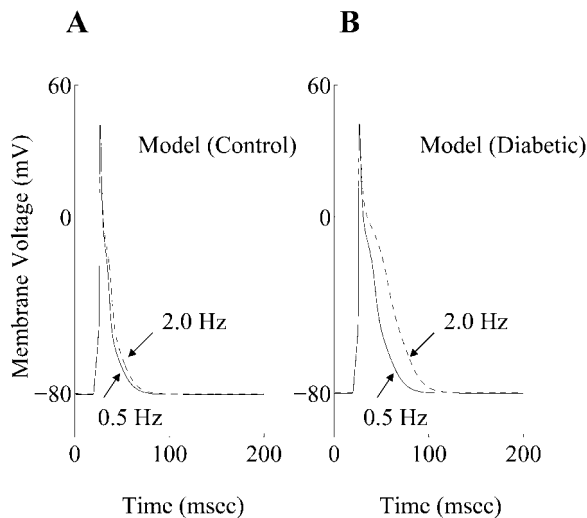
FIGURE 3   Rate dependence of simulated action potentials. (*A*) Steady-state effects of applying stimuli on the control action potential at 0.5 Hz (*solid line*) and 2.0 Hz (*dashed line*). (*B*) Steady-state effects of applying stimuli on the diabetic action potentials at 0.5 Hz (*solid line*) and 2.0 Hz (*dashed line*).

$[Ca^{2+}]_i$ and associated fluxes in control and diabetic cells

The simulated $[Ca^{2+}]_i$ waveforms corresponding to the control and diabetic action potentials are shown in Fig. 6. The diastolic and the peak systolic values of $[Ca^{2+}]_i$ during the simulated control RV action potential (73.34 nM and 330.83 nM) were comparable to corresponding experimental measurements in control RV myocytes, viz. 78.4 $\pm$ 22.6 nM and 401 $\pm$ 115.0 nM respectively (Kaprielian et al., 1999). The peak systolic value of the simulated $[Ca^{2+}]_i$ is reduced by $\approx$5% in the diabetic case (Table 2), although the diastolic values were similar ($\approx$73 nM). This reduction in the peak systolic $[Ca^{2+}]_i$ is in accordance with experimental observations, where the mean peak Ca^{2+} ratio (measurements made using Fura-2) in the diabetic cells was reduced by $\approx$10.0% (Ren and Davidoff, 1997). The simulated Ca^{2+} transient declines more slowly in the diabetic case, as demonstrated in experimental observations (Ren and Davidoff, 1997). The alterations in the I_{CaL} waveform result in a higher influx of Ca^{2+} ions (Q_{CaL}) during the diabetic action potential, compared to the control one (exact values were 15.63 pC and 12.24 pC respectively). Q_{CaL} value for the RV myocyte in the control case is in close agreement with the experimental measurement, 12.4 $\pm$ 1.7 pC (Kaprielian et al., 1999). The net influx of Ca^{2+} ions (via I_{CaL} and I_{Bca}) during an action potential in both the control and diabetic cases is balanced by the Ca^{2+} extrusion via I_{NaCa} during a cardiac cycle (Table 2). This is in accordance with experimental findings regarding the balance of Ca^{2+} ion transfer across the sarcolemma during a cardiac cycle (Bouchard et al., 1995; Clark et al., 1996). The Ca^{2+} content in the junctional SR
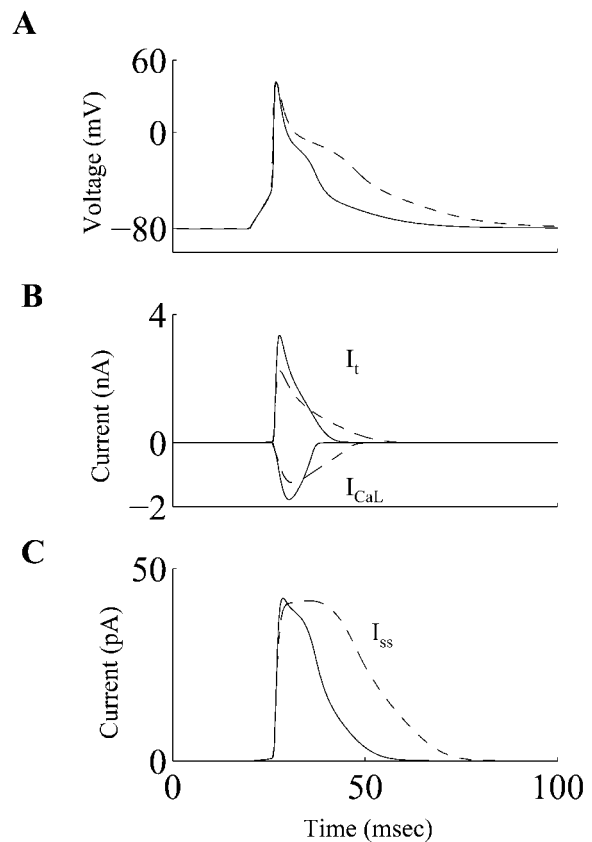

FIGURE 4   (*A*) Simulated action potentials, (*B*) underlying Ca^{2+}-independent transient outward K^+ current (I_t), and the L-type Ca^{2+} current (I_{CaL}), and (*C*) the steady-state outward K^+ current (I_{ss}) during the control (*solid line*) and diabetic (*dashed line*) conditions.

(JSR) just before the application of a stimulus to elicit a simulated action potential in the control RV myocyte was 60.24 μM; this is similar to the recently reported physiological values of SR Ca^{2+} content in rat ventricular myocytes, which were 64.0 $\pm$ 6.0 μM (Trafford et al., 2001) and 56 $\pm$ 7.2 μM (Sah et al., 2001). The JSR Ca^{2+} content was reduced by 26.38% during the diabetic action potential (the absolute value was 44.35 μM). However, the depletion of the JSR during both control and diabetes actions potentials was comparable; JSR was depleted by $\approx$36% and $\approx$39% during control and diabetic action potentials respectively.

DISCUSSION

The main motivation for the development of this model was to gain further quantitative insights concerning the ionic basis of the impaired excitation, repolarization, and E-C coupling processes in myocytes isolated from the ventricle of adult rats exhibiting STZ-induced type-I diabetes. To achieve this, we first derived and validated an approach for simulating the electrophysiological responses and E-C
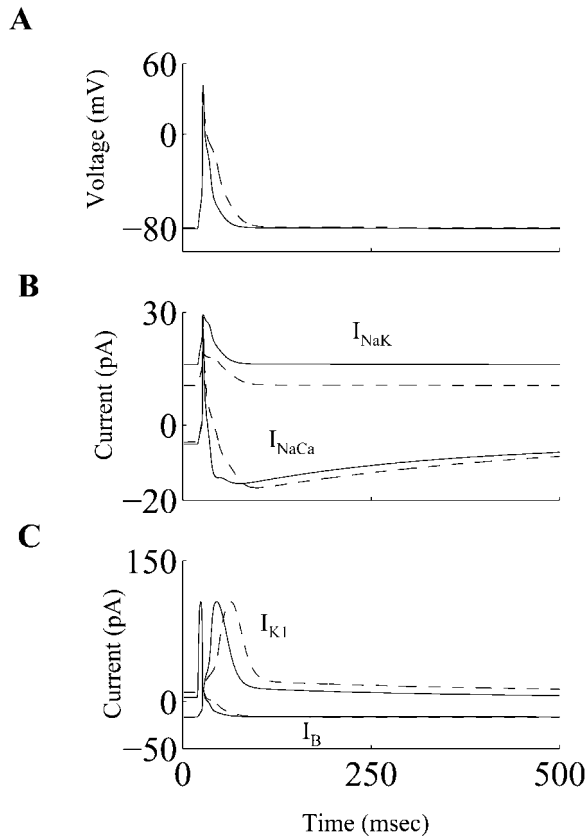
A

B

C

FIGURE 5 (*A*) Simulated action potentials, (*B*) underlying Na$^+$-K$^+$ pump current (I_{NaK}), the Na$^+$-Ca^{2+} exchanger current (I_{NaCa}), and (*C*) the background current (I_B), and the inward rectifier K$^+$ current (I_{K1}) during control (*solid line*) and diabetic (*dashed line*) conditions.
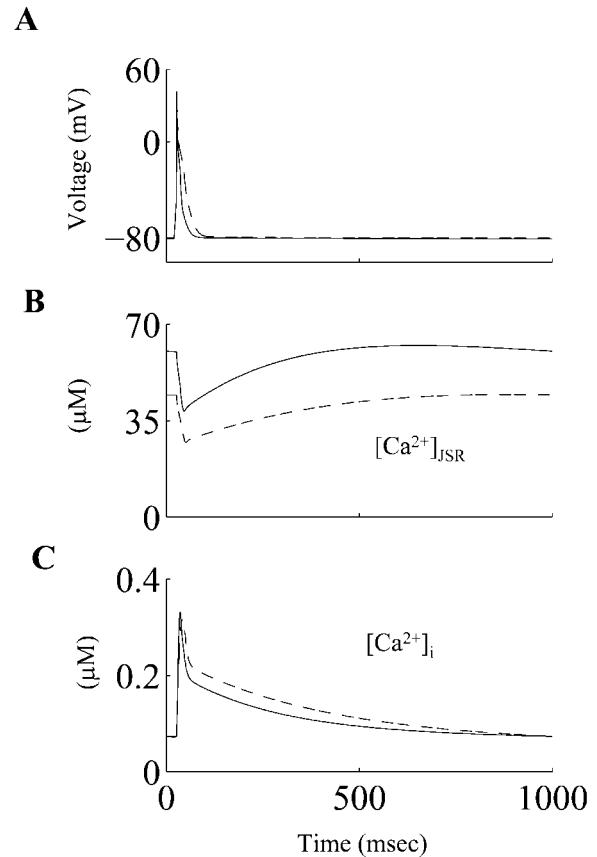
A

B

C

FIGURE 6 (*A*) Simulated action potentials, (*B*) underlying junctional sarcoplasmic reticulum Ca^{2+} load ([Ca^{2+}]$_{JSR}$), and (*C*) the underlying intracellular Ca^{2+} transient ([Ca^{2+}]$_i$) during control (*solid line*) and diabetic (*dashed line*) conditions.

coupling for the normal or control rat RV myocyte. This formulation was then modified to mimic the electrophysiological changes reported for the type-I model of diabetes. The majority of these changes were based on semiquantitative data obtained from patch clamp experiments in STZ-induced diabetic myocytes, or observations in cultured myocytes maintained under hyperglycemic conditions. These were complemented with assumptions based on measurements made in chronic diabetic conditions (when data in acute diabetic conditions was unavailable). The resulting simulations were able to mathematically reconstruct a variety of the electrophysiological changes, which are consistent features of diabetic myocytes. These include: an increased APD, more pronounced rate-dependent APD prolongation, slower dV/dt_{max}, abnormal [Ca^{2+}]$_i$ homeostasis, as well as the small changes in the properties of the quiescent cells (V_{rest}, R_{in}). Our computations illustrate how the diabetic phenotype can result from concomitant changes and complex nonlinear interactions between a number of ion-channel currents (I_t, I_{ss}, I_{CaL}, I_B, I_{Na}), and currents due to the antiporter/pump (I_{NaCa}, I_{NaK}), and SR mechanisms (SR uptake and load).

Action potential duration and inotropy in diabetes

Initial investigations into the ionic basis of the delayed repolarization in myocytes isolated from the short-term, type-I diabetic model in rats showed that the densities of I_t and I_{ss} were reduced (Shimoni et al., 1994; 1995). Recent investigations employing molecular biology techniques have shown that the mRNA levels as well as the protein densities of the K$^+$ channel α-subunits Kv4.2, Kv4.3, and Kv2.1 are

TABLE 2 Simulated sarcolemmal and intracellular calcium fluxes in control and diabetic myocytes from the rat right ventricle

	Q_{CaL} (pC)	Q_{BCa} (pC)	Q_{NaCa} (pC)	[Ca^{2+}]$_{i,rest}$ (nM)	[Ca^{2+}]$_{i,peak}$ (nM)	SR_{rest} (μM)
Control	12.24	4.66	16.07	73.34	330.83	60.24
Diabetic	15.63	2.3	16.96	73.13	316.14	44.35

Q_{CaL}: Calcium influx via I_{CaL} during the action potential; Q_{BCa}: Calcium influx via $I_{B,Ca}$ during the action potential; Q_{NaCa}: Calcium efflux via I_{NaCa} during the action potential; [Ca^{2+}]$_{i,rest}$: Diastolic value of [Ca^{2+}]$_i$ [Ca^{2+}]$_{i,peak}$: Peak systolic value of the Ca^{2+} transient during the action potential; SR_{rest}: JSR Ca^{2+} content during diastole.

downregulated in this acute model of STZ-induced diabetes in rats (Qin et al., 2001). Kv4.2/Kv4.3 α-subunits are thought to encode for I_t (Fiset et al., 1997, Oudit et al., 2001); whereas the Kv2.1 α-subunit along with other α-subunits such as Kv1.5 and Kv3.1/Kv3.2 is thought to underlie the TEA-sensitive K^+ current I_{ss} in rat ventricular myocytes (Nerbonne, 2001; Schultz et al., 2001).

In contrast, the role of changes in I_{CaL} in the diabetic phenotype remains poorly defined. Earlier experiments in chronic diabetes reported no significant changes in I_{CaL} density (Jourdon and Feuvray, 1993); however, more recent studies have suggested that the density of I_{CaL} is down-regulated (Wang et al., 1995; Chattou et al., 1999), and its fast inactivation time constant is slowed (Chattou et al., 1999). When the diabetic action potential in our model was simulated assuming no changes in I_{CaL} properties (not shown), the APD was increased, but the model failed to simulate the reported abnormal changes in $[Ca^{2+}]_i$, despite an impaired SR uptake. In fact, under these conditions/ assumptions, the peak systolic value of $[Ca^{2+}]_i$ was enhanced. Further computational analyses showed that this change in $[Ca^{2+}]_i$ was caused by the increase in APD, which was so large (due to no reduction in the inward current I_{CaL}), that it led to a substantial enhancement of the influx of Ca^{2+} ions via I_{CaL} (increase by $\approx100\%$), when compared to the control case. This behavior is consistent with earlier experimental results (Bouchard et al., 1995; Clark et al., 1996), as well as recent model simulations (Pandit et al., 2001), which demonstrated the mechanistic linkage between an increased APD and increased influx of Ca^{2+} ions. The increased influx was the basis of a larger trigger for calcium induced calcium release (CICR), and subsequently increased the efficiency of SR release (Pandit et al., 2001; Sah et al., 2001), thereby compensating for the impaired SR uptake. The end result was a higher peak systolic value for $[Ca^{2+}]_i$.

However, when the diabetic action potential was simulated by incorporating a reduced density and slower inactivation kinetics of I_{CaL} as well as an impaired SR uptake, the model was able to simultaneously simulate an increased APD and a small decrease in $[Ca^{2+}]_i$ amplitude. For example, a reduction in I_{CaL} density by 24% resulted in a relatively smaller increase in the influx of Ca^{2+} ions during the diabetic action potential (increase by $\approx28\%$). This smaller trigger for CICR, along with an impaired SR uptake, resulted in the peak systolic value for $[Ca^{2+}]_i$ being somewhat smaller during the diabetic action potential (Table 2), which is in accordance with experimental results (Ren and Davidoff, 1997). A reduction in I_{CaL} (an inward current) will also tend to reduce the APD. However, because this reduction was also accompanied by simultaneous reductions in I_t and I_{ss}, along with the slower inactivation of I_{CaL}, the net result was an overall reduction in the outward repolarizing current, thereby prolonging the APD.

Our simulations thus support the hypothesis that changes in the properties of I_{CaL} are essential in explaining the diabetic phenotype (increased APD, reduced $[Ca^{2+}]_i$), and draw attention to the intricate nonlinear interaction between I_t, I_{ss}, I_{CaL}, and SR uptake, which brings about this change.

Rate dependence, excitation, and quiescent properties of ventricular myocytes in type-I diabetes

The recovery from inactivation of I_t in rat model formulations is biphasic in nature, consisting of fast and slow components (Pandit et al., 2001). This is in accordance with experimental observations (Shimoni et al., 1995). The contribution of the slow component to overall inactivation is $\approx11\%$ in the control case, and is enhanced to $\approx31\%$ in the diabetic case. By incorporating the experimentally described slowed recovery in I_t (Shimoni et al., 1994), the model is able to simulate the enhanced prolongation of APD when stimulus frequency was increased from 0.5 Hz to 2.0 Hz under diabetic conditions, compared with the control one (Fig. 3). Interestingly, the fast and slow inactivation variables in the model formulation for I_t have been deemed to represent the contributions of Kv4.2/Kv4.3 and Kv1.4 to I_t respectively (Pandit et al., 2001). The greater contribution of the slower inactivation variable in the diabetic model is in accordance with very recent experimental observations demonstrating that the density of Kv1.4 is substantially enhanced in diabetic conditions (Nishiyama et al., 2001).

Our model also predicts a small decrease ($\approx5\%$) in the upstroke of the diabetic action potential, which has been experimentally observed (Pacher et al., 1999). Our simulations show that the underlying cause for this decrease is the reduction in the availability of the Na^+ channels, due to the small depolarization of V_{rest}. Specifically, the steady-state, half-inactivation voltage of I_{Na} is -76.1 mV; therefore even a small depolarization (0.5–1.0 mV) in V_{rest} can change the Na^+ channel availability. Indeed, experimental evidence shows that there is a decrease in the maximum rate of depolarization in STZ-induced diabetic rats, which increases progressively with development of the disease (Pacher et al., 1999). The lack of any significant change in the peak overshoot of the diabetic action potential, when compared to the control one can be explained by a reduction in I_{Na}, in combination with a simultaneous reduction in I_t. Again, this finding is in accordance with experimental findings, where no significant differences were found in peak overshoot values during chronic diabetes (Casis et al., 2000).

From our quantitative analysis, we note that a small depolarization in V_{rest} (and the subsequent change in R_{in}) can be attributed primarily to a downregulation of the electrogenic pump current, I_{NaK}. Thus, the model is able to replicate the tendency toward depolarization in diabetic myocytes (Shimoni et al., 1994). Interestingly, V_{rest} is also reported to differ significantly in myocytes maintained under hyperglycemic conditions (Ren et al., 1997). V_{rest} was

-77.0 ± 1.0 mV under high glucose conditions, compared to -81.0 ± 1.0 mV in normal conditions (Ren et al., 1997).

Reported effects of PKC can be integrated into this model

Several investigators have provided strong evidence that the subcellular changes in the diabetic heart may be partially due to alterations in the protein kinase C (PKC) activity, and/or PKC-mediated signal transduction mechanisms. In particular, the translocation of εPKC from cystolic to particulate fractions has been described in diabetic myocytes (Koya and King, 1998; Liu et al., 1999). The functional activation of εPKC has been observed in the in vivo, STZ-induced model of diabetes (Malhotra et al., 1997), as well as in myocytes maintained under hyperglycemic conditions (Malhotra et al., 2001). Accordingly, our simulations have incorporated the experimentally observed effects of εPKC on I_{CaL} (Hu et al., 2000) and I_{NaK} (Buhagiar et al., 2001), because the alterations in these currents have not been measured in myocytes isolated from the short-term, in vivo, diabetic model. These changes were necessary in our overall explanation for the abnormal Ca^{2+} homeostasis and changes in V_{rest} observed in the diabetic myocyte experimentally (Shimoni et al., 1994).

The activation of εPKC in hyperglycemic conditions also increases the phosphorylation of troponin I (Malhotra et al., 2001), and cardiac specific over-expression of εPKC is known to increase the myofilament sensitivity to Ca^{2+} ions (Takeishi et al., 2000). Additionally, it has been shown that PKC activation slows inactivation of I_{Na}, which affects the APD_{90} value in rat ventricular myocytes (Ward and Giles, 1997). However it is unclear at the present time whether this mechanism contributes to an APD prolongation in diabetes. Accordingly, these and other reported effects of PKC isoform-specific activation have not been included in the present model formulations. However, they suggest that the contribution of additional ionic mechanisms/biophysical processes to the diabetic phenotype cannot be ruled out.

Limitations

These results and insights from rat ventricular myocytes under diabetic conditions should be extrapolated with caution when attempting to relate them to similar human studies, because the ventricular action potential and the underlying ionic currents are very different in humans and rats. A second limitation of the present study is that the SR Ca^{2+} dynamics have been adapted from a canine common pool model (Winslow et al., 1999). The Ca^{2+} dynamics in rat are now known to be different from their canine counterparts (Bers, 2001). Future modifications that incorporate and validate the model for the specific properties in rat, as well as formulations for a more sophisticated local control model of the Ca^{2+} dynamics will be essential to simulate $[Ca^{2+}]_i$

homeostasis and mechanisms such as graded SR release (Greenstein and Winslow, 2001). A third limitation is that the present model does not account for the changes in the intracellular Na^+ concentration ($[Na^+]_i$), which might occur during prolonged periods of pacing (the present simulation results are illustrated after a train of 20 pulses). Experimental studies have reported both an increase in $[Na^+]_i$ (Warley, 1991), and a decrease in $[Na^+]_i$ (Katoh et al., 1995) during diabetes; thus this important issue remains controversial. Our model also does not incorporate a formulation for the Na^+-H^+ exchanger, which is an important mediator of Na^+ ion influx in rat ventricular myocytes (Despa et al., 2002), and is depressed during diabetes (Pierce et al., 1990). In summary, both experimental ambiguities and modeling limitations prevent the present study from accounting for the changes in $[Na^+]_i$ during long-term pacing. Finally, we note that the changes in I_{CaL} and SR activity in the diabetic model are

Changes in Transmembrane Ionic Currents

$\downarrow I_t$, $\downarrow I_{ss}$, and slower inactivation of I_{CaL}

$\Downarrow$

Result

Prolongation of APD

Changes in Intracellular Ca^{2-} Homeostasis

$\downarrow I_{CaL}$, $\downarrow$ SR Uptake

$\Downarrow$

$\downarrow$ SR Ca^{2+} content

$\Downarrow$

Result

$\downarrow [Ca^{2-}]_{i,peak}$

Changes in Na^+-K^+ Gradients

$\downarrow I_{NaK}$

$\Downarrow$

V_{rest} (depolarized)

$\Downarrow$

Result

Changes in R_{in}, excitability (dV/dt_{max})

FIGURE 7 Diagram summarizing the electrophysiological alterations and their underlying causes as revealed by this mathematical model in the setting of short-term, type-I (insulin dependent), STZ-induced diabetes in rat ventricular myocytes.

based on observations in cultured myocytes and chronic diabetic conditions respectively, because corresponding data from the short-term, STZ-induced model of diabetes in rat are not available. Further experiments are therefore necessary to obtain quantitative data regarding the changes in the intracellular Ca^{2+} dynamics under well-defined type-I diabetic conditions. Thereafter, this aspect of the present modeling effort can and should be improved and updated.

SUMMARY

The results of this model development provide novel insights into the plausible ionic mechanisms that can account for the changes in the action potential profile and the abnormal excitation-contraction coupling in rat ventricular myocytes induced with type-I diabetes. APD prolongation is due to a reduction of the K^+ currents I_t and I_{ss}, along with slowed inactivation of I_{CaL}. The abnormal Ca^{2+} homeostasis (smaller peak, reduced rate of decay) can be attributed to a decreased SR load, which results from a combination of a downregulation in I_{CaL} and an impaired SR uptake. The small depolarization of the resting membrane potential (V_{rest}) is due to a decrease in the Na^+-K^+ pump current. The change in V_{rest} reduces the availability of the Na^+ channels, causing a slower upstroke of the action potential (dV/dt_{max}). These interacting factors are summarized in Fig. 7, which in diagram form present the interdependent biophysical mechanisms for the observed electrophysiological changes, and in that way, highlight potential targets for reversing the diabetic cellular phenotype by means of gene therapy approaches (Trost et al., 2002). A future interesting extension of this study could involve exploring the action potential variations in the rat left ventricle during diabetes and predicting the subsequent changes in T-wave shape, and could be based on a recent modeling study (Gima and Rudy, 2002).

REFERENCES

Ashamalla, S. M., D. Navarro, and C. A. Ward. 2001. Gradient of sodium current across the left ventricular wall of adult rat hearts. *J. Physiol.* 536:439–443.

Bers, D. M. 2001. Excitation-Contraction Coupling and Cardiac Contractile Force. Kluwer Academic Publications.

Bogoyevitch, M. A., P. J. Parker, and P. H. Sugden. 1993. Characterization of protein kinase C isotype expression in adult rat heart. Protein kinase

C-ε is a major isotype present, and it is activated by phorbol esters, epinephrine, and endothelin. *Circ. Res.* 72:757–767.

Bouchard, R. A., R. B. Clark, and W. R. Giles. 1995. Effects of action potential duration on excitation-contraction coupling in rat ventricular myocytes. Action potential voltage-clamp measurements. *Circ. Res.* 76:790–801.

Buhagiar, K. A., P. S. Hansen, N. L. Bewick, and H. H. Rasmussen. 2001. Protein kinase C ε contributes to regulation of the sarcolemmal Na^+-K^+ pump. *Am. J. Physiol. Cell Physiol.* 281:C1059–C1063.

Casis, O., M. Iriarte, M. Gallego, and J. A. Sanchez-Chapula. 1998. Differences in regional distribution of K^+ current densities in rat ventricle. *Life Sci.* 63:391–400.

Casis, O., M. Gallego, M. Iriarte, and J. A. Sanchez-Chapula. 2000. Effects of diabetic cardiomyopathy on regional electrophysiologic characteristics of rat ventricle. *Diabetologia.* 43:101–109.

Chattou, S., J. Diacono, and D. Feuvray. 1999. Decrease in sodium-calcium exchange and calcium currents in diabetic rat ventricular myocytes. *Acta Physiol. Scand.* 166:137–144.

Clark, R. B., R. A. Bouchard, and W. R. Giles. 1996. Action potential duration modulates calcium influx, Na^+-Ca^{2+} exchange, and intracellular calcium release in rat ventricular myocytes. *Ann. N. Y. Acad. Sci.* 779:417–428.

Courtemanche, M., R. J. Ramirez, and S. Nattel. 1999. Ionic targets for drug therapy and atrial fibrillation-induced electrical remodeling: insights from a mathematical model. *Cardiovasc. Res.* 42:477–489.

Davidoff, A. J., and J. Ren. 1997. Low insulin and high glucose induce abnormal relaxation in cultured adult rat ventricular myocytes. *Am. J. Physiol.* 272:H159–H167.

Demir, S. S., J. W. Clark, C. R. Murphey, and W. R. Giles. 1994. A mathematical model of a rabbit sinoatrial node cell. *Am. J. Physiol.* 266:C832–C852.

Demir, S. S., R. J. Butera, A. A. DeFranceschi, J. W. Clark, and J. H. Byrne. 1997. Phase sensitivity and entrainment in a modeled bursting neuron. *Biophys. J.* 72:579–594.

Demir, S. S., J. W. Clark, and W. R. Giles. 1999. Parasympathetic modulation of sinoatrial node pacemaker activity in rabbit heart: a unifying model. *Am. J. Physiol.* 276:H2221–H2244.

Despa, S., M. A. Islam, S. M. Pogwizd, and D. M. Bers. 2002. Intracellular $[Na^+]_i$ and Na^+ pump rate in rat and rabbit ventricular myocytes. *J. Physiol.* 539:133–143.

Dillmann, W. H. 1989. Diabetes and thyroid-hormone-induced changes in cardiac function and their molecular basis. *Annu. Rev. Med.* 40:373–394.

Dutta, K., and A. J. Davidoff. 2000. Na^+/Ca^{2+} exchange is intact in high [glucose]-induced cardiomyopathy. *Biophys. J.* 78:373a (Abstr.)

Ewing, D. J., O. Boland, J. M. Neilson, C. G. Cho, and B. F. Clarke. 1991. Autonomic neuropathy, QT interval lengthening, and unexpected deaths in male diabetic patients. *Diabetologia.* 34:182–185.

Fiset, C., R. B. Clark, Y. Shimoni, and W. R. Giles. 1997. Shal-type channels contribute to the Ca^{2+}-independent transient outward K^+ current in rat ventricle. *J. Physiol.* 500:51–64.

Gima, K., and Y. Rudy. 2002. Ionic current basis of electrocardiographic waveforms: a model study. *Circ. Res.* 90:889–896.

Greenstein, J. L., and R. L. Winslow. 2001. Integration of a stochastic model of local calcium control with a simulation of the cardiac ventricular action potential. *Biophys. J.* 80:593a (Abstract.).

Hu, K., D. Mochly-Rosen, and M. Boutjdir. 2000. Evidence for functional role of εPKC isozyme in the regulation of cardiac Ca^{2+} channels. *Am. J. Physiol. Heart Circ. Physiol.* 279:H2658–H2664.

Jourdon, P., and D. Feuvray. 1993. Calcium and potassium currents in ventricular myocytes isolated from diabetic rats. *J. Physiol.* 470:411–429.

Kaprielian, R., A. D. Wickenden, Z. Kassiri, T. G. Parker, P. P. Liu, and P. H. Backx. 1999. Relationship between K^+ channel down-regulation and $[Ca^{2+}]_i$ in rat ventricular myocytes following myocardial infarction. *J. Physiol.* 517:229–245.

Kato, K., D. C. Chapman, H. Rupp, A. Lukas, and N. S. Dhalla. 1999. Alterations of heart function and Na^+-K^+-ATPase activity by etomoxir in diabetic rats. *J. Appl. Physiol.* 86:812–818.

Katoh, H., N. Noda, H. Hayashi, H. Satoh, H. Terada, R. Ohno, and N. Yamazaki. 1995. Intracellular sodium concentration in diabetic rat ventricular myocytes. *Jpn. Heart J.* 36:647–656.

Koya, D., and G. L. King. 1998. Protein kinase C activation and the development of diabetic complications. *Diabetes.* 47:859–866 (Review.).

Liu, X., J. Wang, N. Takeda, L. Binaglia, V. Panagia, and N. S. Dhalla. 1999. Changes in cardiac protein kinase C activities and isozymes in streptozotocin-induced diabetes. *Am. J. Physiol.* 277:E798–E804.

MacDonell, K. L., D. L. Severson, and W. R. Giles. 1998. Depression of excitability by sphingosine 1-phosphate in rat ventricular myocytes. *Am. J. Physiol.* 275:H2291–H2299.

Mahgoub, M. A., and A. S. Abd-Elfattah. 1998. Diabetes mellitus and cardiac function. *Mol. Cell. Biochem.* 180:59–64.

Malhotra, A., D. Reich, A. Nakouzi, V. Sanghi, D. L. Geenen, and P. M. Buttrick. 1997. Experimental diabetes is associated with functional activation of protein kinase C epsilon and phosphorylation of troponin I in the heart, which are prevented by angiotensin II receptor blockade. *Circ. Res.* 81:1027–1033.

Malhotra, A., B. P. Kang, S. Cheung, D. Opawumi, and L. G. Meggs. 2001. Angiotensin II promotes glucose-induced activation of cardiac protein kinase C isozymes and phosphorylation of troponin I. *Diabetes.* 50:1918–1926.

Nerbonne, J. M. 2001. Molecular analysis of voltage-gated K^+ channel diversity and functioning in the mammalian heart. *In* Handbook of Physiology: The Cardiovascular System. E. Page, H. A. Fozzard, and R. J. Solaro, editors. Oxford University Press, Oxford 568–594.

Netticadan, T., R. M. Temsah, A. Kent, V. Elimban, and N. S. Dhalla. 2001. Depressed levels of Ca^{2+}-cycling proteins may underlie sarcoplasmic reticulum dysfunction in the diabetic heart. *Diabetes.* 50:2133–2138.

Nishiyama, A., D. N. Ishii, P. H. Backx, B. E. Pulford, B. R. Birks, and M. M. Tamkun. 2001. Altered K^+ channel gene expression in diabetic rat ventricle: isoform switching between Kv4.2 and Kv1.4. *Am. J. Physiol. Heart Circ. Physiol.* 281:H1800–H1807.

Noble, D. 2002. Modeling the heart–from genes to cells to the whole organ. *Science.* 295:1678–1682.

Oudit, G. Y., Z. Kassiri, R. Sah, R. J. Ramirez, C. Zobel, and P. H. Backx. 2001. The molecular physiology of the cardiac transient outward potassium current I_{to} in normal and diseased myocardium. *J. Mol. Cell. Cardiol.* 33:851–872.

Pacher, P., Z. Ungvari, P. P. Nanasi, and V. Kecskemeti. 1999. Electrophysiological changes in rat ventricular and atrial myocardium at different stages of experimental diabetes. *Acta Physiol. Scand.* 166:7–13.

Pandit, S. V., R. B. Clark, W. R. Giles, and S. S. Demir. 2001. A mathematical model of action potential heterogeneity in adult rat left ventricular myocytes. *Biophys. J.* 81:3029–3051.

Pierce, G. N., B. Ramjiawan, N. S. Dhalla, and R. Ferrari. 1990. Na^+-H^+ exchange in cardiac sarcolemmal vesicles isolated from diabetic rats. *Am. J. Physiol.* 258:H255–H261.

Qin, D., B. Huang, L. Deng, H. El-Adawi, K. Ganguly, J. R. Sowers, and N. El-Sherif. 2001. Downregulation of K^+ channel genes expression in type I diabetic cardiomyopathy. *Biochem. Biophys. Res. Commun.* 283:549–553.

Ren, J., and A. J. Davidoff. 1997. Diabetes rapidly induces contractile dysfunctions in isolated ventricular myocytes. *Am. J. Physiol.* 272:H148–H158.

Ren, J., G. A. Gintant, R. E. Miller, and A. J. Davidoff. 1997. High extracellular glucose impairs cardiac E-C coupling in a glycosylation-dependent manner. *Am. J. Physiol.* 273:H2876–H2883.

Robillon, J. F., J. L. Sadoul, S. Benmerabet, L. Joly-Lemoine, A. Fredenrich, and B. Canivet. 1999. Assessment of cardiac arrhythmic risk in diabetic patients using QT dispersion abnormalities. *Diabetes Metab.* 25:419–423.

Rudy, Y. 2000. From genome to physiome: integrative models of cardiac excitation. *Ann. Biomed. Eng.* 28:945–950.

Rybin, V. O., and S. F. Steinberg. 1994. Protein kinase C isoform expression and regulation in the developing rat heart. *Circ. Res.* 74: 299–309.

Sah, R., R. J. Ramirez, R. Kaprielian, and P. H. Backx. 2001. Alterations in action potential profile enhance excitation-contraction coupling in rat cardiac myocytes. *J. Physiol.* 533:201–214.

Schultz, J. H., T. Volk, and E. Ehmke. 2001. Heterogeneity of Kv2.1 mRNA expression and delayed rectifier current in single isolated myocytes from rat left ventricle. *Circ. Res.* 88:483–490.

Shimoni, Y., L. Firek, D. Severson, and W. R. Giles. 1994. Short-term diabetes alters K^+ currents in rat ventricular myocytes. *Circ. Res.* 74:620–628.

Shimoni, Y., D. Severson, and W. R. Giles. 1995. Thyroid status and diabetes modulate regional differences in potassium currents in rat ventricle. *J. Physiol.* 488:673–688.

Shimoni, Y., P. E. Light, and R. J. French. 1998. Altered ATP sensitivity of ATP-dependent K^+ channels in diabetic rat hearts. *Am. J. Physiol.* 275:E568–E576.

Shimoni, Y. 1999. Protein kinase C regulation of K^+ currents in rat ventricular myocytes and its modification by hormonal status. *J. Physiol.* 520:439–449.

Standl, E., and O. Schnell. 2000. A new look at the heart in diabetes mellitus: from ailing to failing. *Diabetologia.* 43:1455–1469.

Takeishi, Y., P. Ping, R. Bolli, D. L. Kirkpatrick, B. D. Hoit, and R. A. Walsh. 2000. Transgenic overexpression of constitutively active protein kinase C ε causes concentric cardiac hypertrophy. *Circ. Res.* 86:1218–1223.

Trafford, A. W., M. E. Diaz, and D. A. Eisner. 2001. Coordinated control of cell Ca^{2+} loading and triggered release from the sarcoplasmic reticulum underlies the rapid inotropic response to increased L-type Ca^{2+} current. *Circ. Res.* 88:195–201.

Trost, S. U., D. D. Belke, W. F. Bluhm, M. Meyer, E. Swanson, and W. H. Dillmann. 2002. Overexpression of the sarcoplasmic reticulum Ca^{2+}-ATPase improves myocardial contractility in diabetic cardiomyopathy. *Diabetes.* 51:1166–1171.

Wang, D. W., T. Kiyosue, S. Shigematsu, and M. Arita. 1995. Abnormalities of K^+ and Ca^{2+} currents in ventricular myocytes from rats with chronic diabetes. *Am. J. Physiol.* 269:H1288–H1296.

Ward, C. A., and W. R. Giles. 1997. Ionic mechanism of the effects of hydrogen peroxide in rat ventricular myocytes. *J. Physiol.* 500:631–642.

Ward, C. A., Z. Ma, S. S. Lee, and W. R. Giles. 1997. Potassium currents in atrial and ventricular myocytes from a rat model of cirrhosis. *Am. J. Physiol.* 273:G537–G544.

Warley, A. 1991. Changes in sodium concentration in cardiac myocytes from diabetic rats. *Scanning Microsc.* 5:239–244.

Watanabe, T., L. M. Delbridge, J. O. Bustamante, and T. F. McDonald. 1983. Heterogeneity of the action potential in isolated rat ventricular myocytes and tissue. *Circ. Res.* 52:280–290.

Winslow, R. L., J. Rice, S. Jafri, E. Marban, and B. O'Rourke. 1999. Mechanisms of altered excitation-contraction coupling in canine tachycardia-induced heart failure, II: model studies. *Circ. Res.* 84:571–586.

Winslow, R. L., D. F. Scollan, A. Holmes, C. K. Yung, J. Zhang, and M. S. Jafri. 2000. Electrophysiological modeling of cardiac ventricular function: from cell to organ. *Annu. Rev. Biomed. Eng.* 2:119–155.

Zhong, Y., S. Ahmed, I. L. Grupp, and M. A. Matlib. 2001. Altered SR protein expression associated with contractile dysfunction in diabetic rat hearts. *Am. J. Physiol. Heart Circ. Physiol.* 281:H1137–H1147.